Catalysis Today 139 (2008) 214–220

Contents lists available at ScienceDirect

Catalysis Today

journal homepage: www.elsevier.com/locate/cattod

A DFT study of methanol dissociation on isolated vanadate groups

L. Gracia [a], P. González-Navarrete [a], M. Calatayud [b,*], J. Andrés [a]

[a] Departament de Química Física i Analítica, Universitat Jaume I, Castelló de La Plana, Spain
[b] Laboratoire de Chimie Théorique LCT, UMR CNRS 7616, Univ. Paris 06, Case 137, 4, Place Jussieu, 75252 Paris, France

ARTICLE INFO

Article history:
Available online 21 July 2008

Keywords:
B3LYP
Vanadium oxide
Methanol
Methoxy
Hydroxyl
ELF

ABSTRACT

Molecular and dissociative adsorption processes of methanol on isolated vanadate groups have been studied by means of density functional theory calculation at the B3LYP computing level. The catalyst is represented by an isolated vanadia unit in two environments: hydrated and supported. First, a $OV(OH)_3$ model considers hydrated conditions and second, a $OV(OTiO_2H)_3$ cluster accounts for the titania-supported site. The stationary points on the potential energy surface have been characterized and their geometries, relative energies and also the vibrational spectra have been obtained. In addition, the nature of chemical bonding has been highlighted by means of the analysis of the electron localization function. Our results show that methanol dissociation is a favourable process leading to methoxide groups. The molecular mechanism for dissociation on V–OH or supported V–O–Ti sites is preferred to that involving vanadyl V=O groups. Hydrogen bonding plays a key role stabilizing molecular methanol intermediates in hydrated conditions, while electrostatic acid/base interactions prevail in supported systems. Our calculated vibrational spectra confirm the experimental band assignment. An ELF bonding analysis identifies the ionic character of catalyst–methanol interactions. A moderate charge transfer of −0.34 electrons to the methoxy group would result in a blue-shift of the vanadyl band.

1. Introduction

Chemical reactions involving methanol are important in many fields including biological processes, fuel cells and catalysis. This molecule is often taken as a probe to map out the catalyst properties on oxide catalyst surfaces [1]. The selective oxidation of methanol to formaldehyde occurring on vanadium oxide supported catalysts is of special interest [2–5]. In these experiments, the molecule first dissociates on the surface and oxidizes to formaldehyde at higher temperatures. Two species, a methanol molecule coordinated to a Lewis metal site, and a dissociated surface methoxy, are found to play a crucial role in supported metal oxide catalyzed reactions. It is estimated that 10% of the surface species are in a molecular form, and 90% of methanol is dissociated as methoxy groups [2,3].

Methanol molecules and methoxy groups are key intermediates that have been detected by different experimental techniques (see ref. [2] and references therein). They are at the origin of the selective oxidation to formaldehyde, but also might lead to undesired products such as dimethyl-ether by recombination. Moreover, the adsorption of methanol on supported metal oxides might be used for the quantification of active sites on such materials [3]. It is thus of great importance to understand their chemical behaviour at the molecular level in catalytic conditions so as to control the key factors leading to the selected products.

Theoretical studies provide relevant insights into the molecular mechanism for methanol oxidation on vanadium-based systems. In the last years the isolated vanadate species have been modelled as supported on silica, titania and zirconia [6–9]. Also, gas-phase neutral and charged clusters have been proven to bring fundamental understanding on the key intermediates and reaction barriers for methanol transformation in oxidation/reduction products [6,10–13]. However, little attention has been paid to the role of the hydroxyl groups present in the real catalysts. For this reason, the presence of hydroxyl groups will be explicitly included in the present work. In addition, the support effect will be treated by considering a titania-supported catalyst. We hope to contribute to a better understanding of the structure, energetic and bonding properties of vanadium oxide catalysts.

In this paper the molecular mechanism for methanol dissociation will be investigated by means of density functional theory (DFT). Two models are investigated to represent the adsorption process. First, a $OV(OH)_3$ model explicitly considers hydrated conditions where surface hydroxyl groups are present. Second, a $OV(OTiO_2H)_3$ cluster is used to represent titania-supported catalysts. The paths leading to methanol dissociation will be discussed for both

* Corresponding author. Tel.: +33 1 44 27 26 82; fax: +33 1 44 27 41 17.
E-mail address: calatayu@lct.jussieu.fr (M. Calatayud).

0920-5861/$ – see front matter © 2008 Elsevier B.V. All rights reserved.
doi:10.1016/j.cattod.2008.05.033

situations. The possible intermediates will be characterized at 0 K and 650 K. Calculated vibrational spectra for all the intermediates will be reported and compared to available experimental results. Finally, the nature of the chemical bonding in selected structures will be described by means of the topological analysis of the electron localization function (ELF) [14].

2. Computational details and model system

All calculations were performed using the Gaussian 03 package [15]. DFT in its three-parameter hybrid unrestricted B3LYP functional [16,17] together with the standard all electron 6-311G(2d,p) [18] basis sets were used in the structural optimization for stationary points. This methodology has been successfully applied to calculate the complex molecular mechanisms associated with the reactions of VO_2^+ with saturated and unsaturated hydrocarbons [19–22] providing accurate results for geometrical and energetic values. The computed stationary points (minima and TSs) have been characterized analyzing the vibrational normal modes after diagonalization of the Hessian matrix, and employing the Berny algorithm for the geometry optimizations [23]. The intrinsic reaction coordinate (IRC) procedure [24,25] has been used to describe minimum energy paths from TSs to the corresponding minima along the imaginary mode of vibration using the algorithm developed by González and Schlegel [26] in the mass-weighted internal coordinate system.

Free energy calculations were performed for each intermediate using standard relationships from statistical mechanics [27–30]. These calculations were done at 650 K, the temperature at which the selective oxidation of methanol to formaldehyde was studied experimentally [8]. Calculations show that the processes are endergonic. Free energy calculations at lower temperatures show that the process is reversed. At 650 K, the adsorbed species of the entrance channel lie above the reference systems. However, this fact can be reversed at lower temperature. In this sense, we have carried out preliminary calculations at 298 K and the results show that at room temperature the adsorbed species and the separate fragments have similar ΔG values.

A bonding analysis is carried out in order to elucidate the nature of the chemical bonds present in the intermediates. Ionic and covalent interactions can be unambiguously identified, and charge transfer processes can be quantitatively determined. Such analysis relies upon a gradient field analysis of the ELF function, $\eta(\mathbf{r})$, of Becke and Edgecombe [31], as proposed by Silvi and Savin [14]. This methodology allows a description of the chemical bond from a rigorous mathematical point of view. An exploration of the mathematical properties of the ELF function enables a partition of the molecular position space in basins of attractors, which present a one to one correspondence with chemical local objects such as bonds and lone pairs. These basins are either core basins, C(X), or valence basins, V(X,...), belonging to the outermost shell and characterized by their coordination number with core basins, which is called the synaptic order. From a quantitative point of view the method allows the integration of the electron density over the basins to provide the basin populations, $\bar{N}$, allowing a quantification of charge transfer phenomena. ELF calculations have

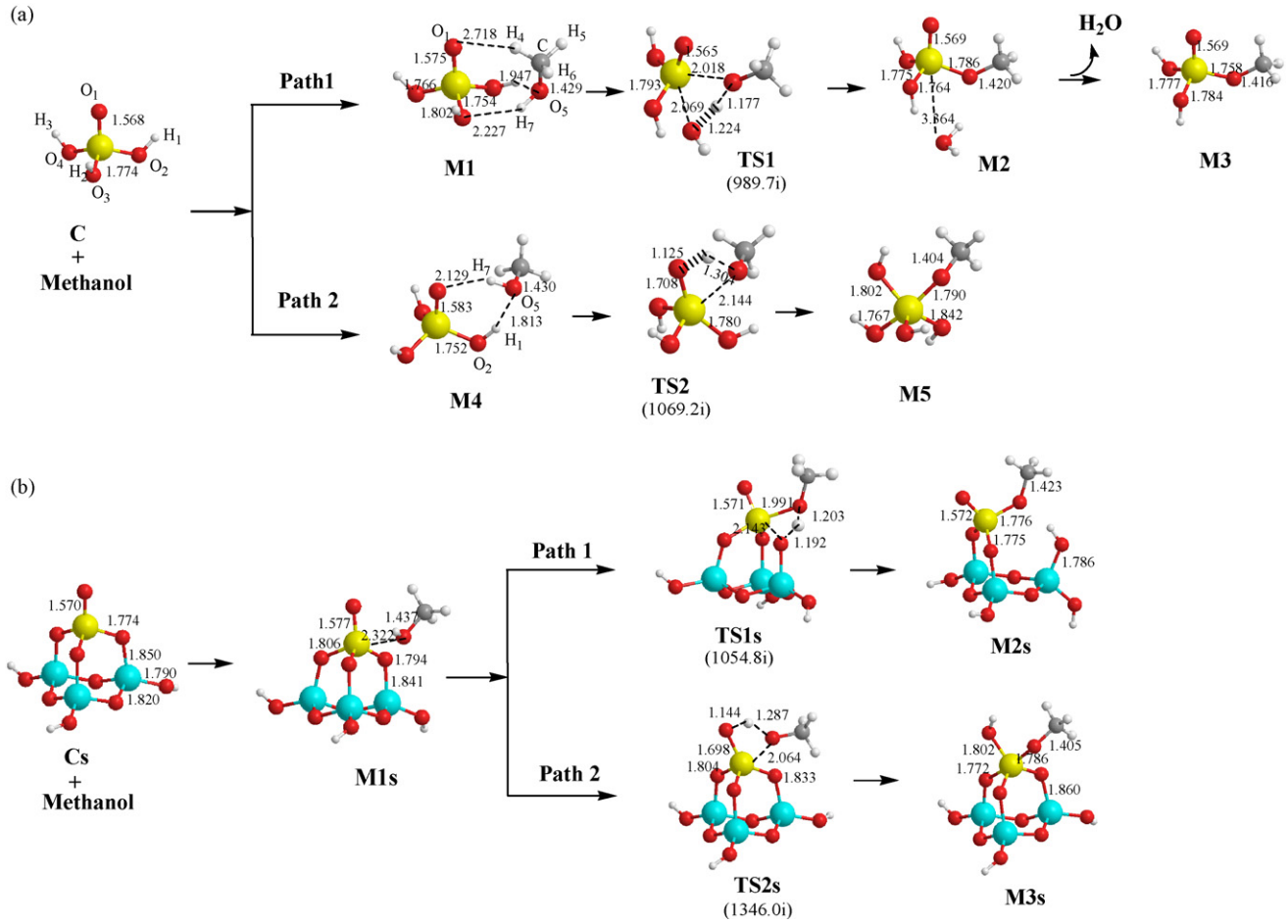

Fig. 1. Structures (distances in Å) of the stationary points found at B3LYP/6-311G(2d,p) level. For TSs, the imaginary vibrational frequencies (cm^{-1}) are shown in parenthesis.

been performed with the TopMod package [32] and isosurfaces have been visualized with the program Amira [33].

Isolated vanadia units show a pyramidal VO_4 structure with a short vanadyl V=O and three equivalent V–O–$M_{support}$ sites. Two models for isolated vanadia catalytic sites are proposed: (i) a hydrated model, $OV(OH)_3$, where the vanadium oxide contains one terminal mono-oxo V=O bond and three terminal hydroxyl groups (representing real catalyst under wet conditions), and (ii) a TiO_2-supported vanadia model, where the vanadium oxide contains the terminal V=O bond and three V–O–Ti, each Ti atom connected to a hydroxyl group and to a bridging O atom between two Ti atoms. The vanadium site possesses in these clusters an oxidation state of V, in a tetrahedral environment which is the common situation in dispersed catalysts. Although alternative models have been proposed [34], the pyramid arrangement seems to be the most generally assumed. The catalyst models are depicted in Fig. 1, referred to in the following as (i) hydrated model (C), with V=O and V–OH distances of 1.568 Å and 1.774 Å, respectively and (ii) supported model (Cs), with V=O and V–O–Ti distances of 1.570 Å and 1.774–1.850 Å, respectively.

3. Results and discussion

The main goal of the present work is to study and characterize the first-stages associated to the interaction of methanol with the catalyst to get fundamental insights into the main properties controlling the reactivity. The stationary points on potential energy surface have been characterized and the role of the vanadyl V=O and the V–OH/V–O–Ti sites is discussed below.

3.1. Reaction paths

There are two possible reaction pathways depending on the adsorption mode of the methanol molecule to the catalyst: Path 1 involves interaction with the hydroxyl group or V–O–Ti site for the hydrated and supported models, respectively, while in the Path 2 the interaction takes place with the vanadyl group. These two alternatives are displayed in Fig. 1. Figs. 2 and 3 show the total energy and free energy profiles at 650 K for the two pathways for both models.

3.1.1. Methanol adsorption

The first step in the mechanism is the formation of a reaction complex. It is well known that the interaction of one methanol molecule with the catalyst surface is favourable [2,3] and it can be associated to weak electrostatic interactions between the vanadium site (acidic) and the oxygen atom in the methanol molecule (basic).

An analysis of the results shows that for the hydrated model the presence of hydrogen bonds between the methanol and the catalyst hydroxyls is responsible for the stabilization of the adsorption process along Path 1; in this pyramidal model the vanadium site is not accessible and the interaction is mainly via hydrogen bonds (see **M1**). The formation process of this complex is favourable by 9.6 kcal/mol, and endergonic at 650 K (13.3 kcal/mol). Along Path 2 the adsorption of methanol to the hydrated cluster is stabilized by the formation of two hydrogen bonds between the methanol OH group: one with the vanadyl fragment and a second one with the catalyst hydroxyl group, forming the reactive complex **M4**. This interaction is more stabilizing than in Path 1 by ~3 kcal/mol for both total and free energy profiles.

In the case of the supported model, the interaction methanol–catalyst takes place by an acid/base electrostatic interaction between the methanol oxygen and the vanadium site (V–$O_{methanol}$ distance of 2.322 Å). The formation process of this complex, **M1s**, is

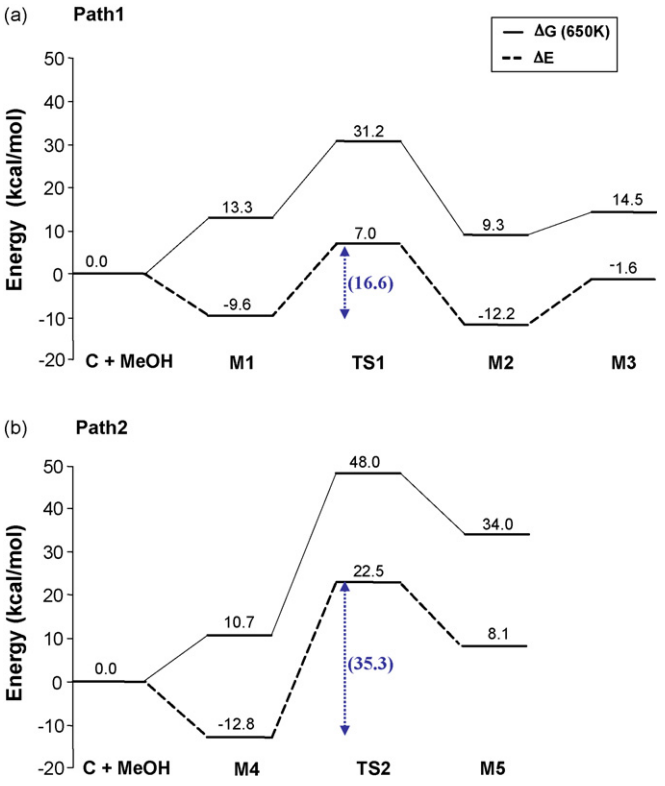

Fig. 2. Total and free energy profiles in kcal/mol, relative to the reactants, at B3LYP/6-311G(2d,p) level for the hydrated model. (a) Path 1, (b) Path 2. In parentheses, the values for the barriers (total energy).

less exothermic compared to **M1** (by 0.9 kcal/mol) and **M4** (by 3.1 kcal/mol) of the hydrated model; and it is an endergonic stage at 650 K (18.9 kcal/mol). The presence of molecular adsorbed methanol has been reported on supported metal oxide catalysts. In these experiments [3], the samples are exposed to methanol at a temperature of 110 °C. At lower temperatures the methanol forms strongly bound methoxy as well as weakly physisorbed molecules, while at higher temperatures the methoxylated surface species react to form formaldehyde and other products.

Therefore, while in the hydrated model the interaction mainly takes place via hydrogen bonds, in the supported model case the metal site is available favouring Lewis acid–base interactions [35].

3.1.2. Methanol dissociation

Subsequently, methanol dissociates into CH_3O^- and H^+; methoxide group binds to the vanadium site and proton is transferred to a catalyst oxygen site. Two alternatives are possible: (i) H^+ transfer to an V–OH group giving a water molecule in the hydrated model, and to an O–$Ti_{support}$ site in the supported model (Path 1) or (ii) H^+ transfer to the V=O group (Path 2), see Fig. 1.

In Path 1 for the hydrated model the transition state **TS1** is associated to both methanol OH group and the V–OH bond breaking processes and the formation of V–OCH_3 and H–OH bonds. In this stationary point the vanadium atom is five-fold coordinated with a V–OCH_3 distance of 2.018 Å, and a H–OCH_3 distance of 1.117 Å. The total (and free) energy barriers for this process are 16.6 (17.9) kcal/mol. In an analogous way, methanol dissociation along Path 1 in the supported model proceeds via **TS1s**, associated to a V–$O_{support}$ breaking process and the formation of the V–OCH_3 and H–$O_{support}$ bonds. As in **TS1**, the oxygen atom of vanadyl fragment as well as the V–OCH_3 interaction are strengthened while V–$O_{support}$ bond is weakened to reach a distance value of 2.143 Å

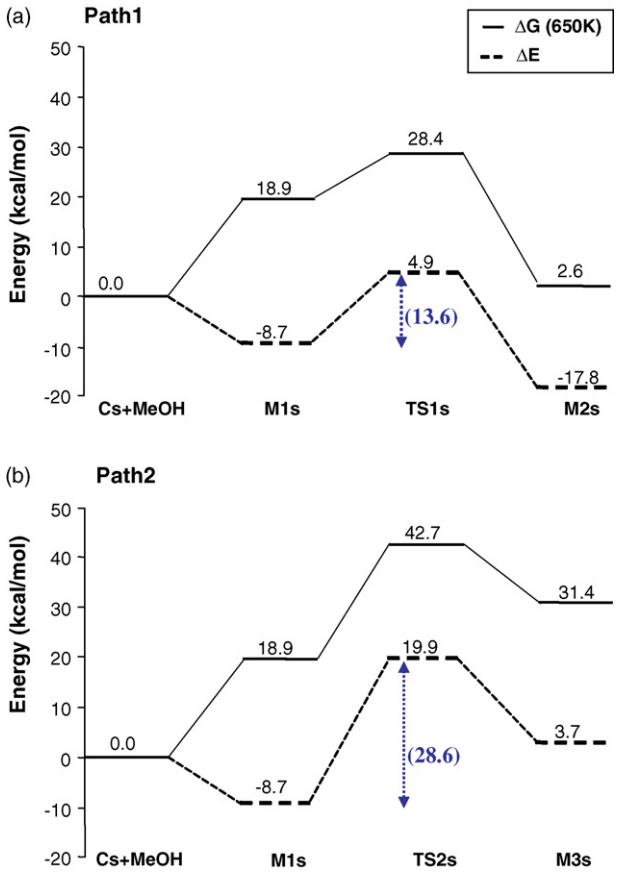

Fig. 3. Total and free energy profiles, relative to the reactants, at B3LYP/6-311G(2d,p) level for the supported model. (a) Path 1, (b) Path 2. In parentheses, the values for the barriers (total energy).

along the proton transfer process. The total (and free) energy barriers for this process are lower than for the hydrated model, 13.6 (10.7) kcal/mol.

For the Path 2, the total (and free) energy barriers are higher than in Path 1 regardless of the catalyst model: 35.3 (37.3) kcal/mol and 28.6 (23.8) kcal/mol, for the hydrated and supported models, respectively. The corresponding transition states **TS2** and **TS2s** involve the cleavage of the short vanadyl V=O bond and the formation of V–OCH_3 and both show longer distances V–OCH_3 (2.144 Å and 2.064 Å, respectively) and H–OCH_3 (1.304 Å and 1.287 Å, respectively) compared to **TS1** and **TS1s**, respectively. The fact that the proton is transferred to the vanadyl group destabilizes the structure compared to **TS1** and **TS1s**, and therefore the mechanism along Path 1 would be preferred to Path 2 for both models.

3.1.3. Methoxy intermediates

From the transition states the methoxy intermediates are reached in which this group is strongly bound to the vanadium site. **TS1** leads to the formation of a weakly bound water molecule, while **TS1s** lead to the break of a V–$O_{support}$ bond by the formation of a HO–$Ti_{support}$ fragment. Along Path 2, both **TS2** and **TS2s** involve the formation of hydroxyl groups.

In the Path 1, the hydrated **M2** intermediate is highly stabilized due to the formation of a water molecule that might desorb. The supported **M2s** structure represents the hydroxylation of the support. In both cases, the vanadium site preserves its initial tetrahedral coordination. The methoxy containing species **M2** and **M2s**, are stabilized by −12.2 kcal/mol and −17.8 kcal/mol, respectively (9.3 kcal/mol and 2.6 kcal/mol at 650 K). This means that the dissociation of methanol is thermodynamically favoured with respect to the molecular interaction. In the hydrated model, the loss of this water molecule to give **M3** destabilizes the complex by 10.6 kcal/mol at 0 K (5.2 kcal/mol at 650 K).

Along Path 2 the proton transfer to the vanadyl oxygen leads to the formation of **M5** and **M3s** in the hydrated and supported models, respectively. In these intermediates the vanadium site is five-fold coordinated, which destabilizes the corresponding complexes by 20.9 kcal/mol and 12.4 kcal/mol, respectively (23.3 kcal/mol and 12.5 kcal/mol at 650 K) with regard to the molecular adsorption.

These results show that the methanol interaction with the catalyst is of different nature regarding the hydration conditions: hydrogen bonding is preferred in hydrated catalysts while acid/base interaction takes place in titania-supported systems. Tetrahedral environment is favoured with respect to five-fold coordinated vanadium. The paths involving the vanadyl V=O group are clearly unfavourable as regards methanol dissociation. Titania-supported model exhibit low barriers indicating a strong effect of the support.

3.2. Vibrational spectra

In order to characterize the possible intermediates we have calculated the harmonic vibrational spectra for all the species considered. We will focus on the methanol fragment. The main frequencies and the band assignment are shown in Table 1 for both hydrated and supported models. As it is well known, density-functional based calculations give overestimated frequencies, especially for stretching modes. For this reason we have applied a correction factor of 0.96 to the computed values, otherwise it is specified in the text.

For the hydrated model, the molecular methanol species (systems **M1**, **M4**) and for supported model (**M1s**) show bands assigned to CH_3 stretching modes υ_{CH} in the region of 2966 cm^{-1} and 2978 cm^{-1} (asymmetric) to 2887 cm^{-1} and 2911 cm^{-1} (symmetric), for **M1** and **M1s**, respectively, in agreement with

Table 1
Calculated and experimental vibrations (in cm^{-1}) for methanol interaction with isolated vanadates

		Molecular				Dissociated				
		Unsupported	Supported **M1s**	[3]	[2]	Unsupported	Supported **M2s**	Supported **M3s**	[3]	[2]
υ_{CH}	Asymmetric	2966	2978	2995–2965	2956–2945	2958	2963	2913	2975	2939–2929
	Symmetric	2887	2911	2965–2953	2850–2833	2885	2895	2860	2935	2850–2833
δ_{CH}	Asymmetric	1446	1435	∼1450	1460–1463	1434	1431	1421	1415	1435
	Symmetric	1420	1410	∼1430		1414	1412	1399		
δ_{OH}		1359	1351*	1370						
υ_{CO}		1042*	1022*	1124–1065		1085*	1081*	1083*		

The calculated values for the hydrated model correspond to the average of similar structures (**M1** and **M4** for molecular methanol and **M2**, **M3** and **M5** for the dissociated methanol). Experimental results are given for supported catalysts. A correction factor of 0.96 is applied for the computed frequencies with the exception of all the υ_{CO} and one δ_{OH} values labelled as (*).

experimental data on supported oxides (see Table 1). Note that the position of the bands observed experimentally oscillates 20–30 cm^{-1} depending on the support used. The difference between the asymmetric and the symmetric modes is calculated to be of 80 cm^{-1} and is consistent with the experimental shift of 100 cm^{-1}. Bending δ_{CH} modes are calculated to vibrate at values of 1446 cm^{-1} and 1435 cm^{-1} (asymmetric) and 1420 cm^{-1} and 1410 cm^{-1} (symmetric) for hydrated and supported models, respectively. Burcham et al. [3] report values of 1450 cm^{-1} and 1430 cm^{-1}. Bronkema et al. [2] report similar values of 1435–1436 cm^{-1}. The methanol OH bending δ_{OH} is found to vibrate at 1359 cm^{-1} and 1351 cm^{-1}, respectively, in good agreement with the results of Burcham et al. (1370 cm^{-1}). The computed C–O stretching vibration is 1042 cm^{-1} and 1022 cm^{-1} for the hydrated and supported models, respectively. These values are lower than the values reported by Burcham et al. (1065–1124 cm^{-1}). For this reason we have not applied any correction factor to this value.

Dissociated methanol is considered in structures **M2**, **M3** and **M5** (hydrated) and **M2s M3s** (supported). The methoxy fragment shows vibrations ~15 cm^{-1} lower than the corresponding molecular interaction. Thus, the methyl bending modes are found to be 2958 cm^{-1} (hydrated), 2963–2913 cm^{-1} (supported), consistent with the experimental values of 2975–2935 cm^{-1} [3] and 2939–2833 cm^{-1} [2]. The same behaviour is observed for the bending modes δ_{CH} with a decrease of ~10 cm^{-1} with respect to the values of the molecularly adsorbed methanol. The C–O stretching band appears in our calculations at 40–60 cm^{-1} higher in energy than the molecular species, which is in the range of the observed peaks reported by Burcham et al [3].

Burcham et al. [3] and Bronkema et al. [2] report a band at 1612 cm^{-1} and 1640 cm^{-1}, respectively, assigned to the bending δ(H–O–H) mode of strongly Lewis-bound water. Our results for model **M2**, containing a water molecule interacting with the vanadium site, predict a weak band for 1610 cm^{-1} (corrected with the 0.96 factor) thus confirming the nature of the species detected in the experiments. Indeed, the band observed at 1612 cm^{-1} is present on the supported catalysts even at 200 °C, indicating a strong interaction, although it is generally displaced by methanol.

A fingerprint of vanadium oxide-based systems is the stretching of the vanadyl V=O group that occurs at 1050 cm^{-1}. In our models this band appears at lower values of wavenumbers for the molecular methanol complexes (1085 cm^{-1} for **M1**, 1056 cm^{-1} for **M4** and 1098 cm^{-1} for **M1s**) than for the dissociated systems (1131 cm^{-1} for **M2**, 1126 cm^{-1} for **M3** and 1112 cm^{-1} for **M2s**) indicating an electronic rearrangement induced by the methoxy groups (see below). Structures **M5** and **M3s** do not show this spectral feature as corresponding to the absence of vanadyl group.

In summary, the calculated frequencies are in agreement with the experimental values and allow to confirm the previous assignments on an *ab-initio* basis. The main features of the vibrational spectra can be reproduced and explained with a simple computational model for hydrated and titania-supported catalysts.

3.3. ELF analysis

ELF isosurface diagrams for the reactant complexes and methoxy intermediates for the hydrated model are presented in Fig. 4. From these diagrams the nature of the chemical bond can be visually deduced: the presence of a disynaptic basin (green button labelled $V(C,O_5)$) indicates a pair of electrons in this region, and thus a covalent bond; its absence indicates a mainly electrostatic interaction. For a finer analysis, in Table 2 the topological population

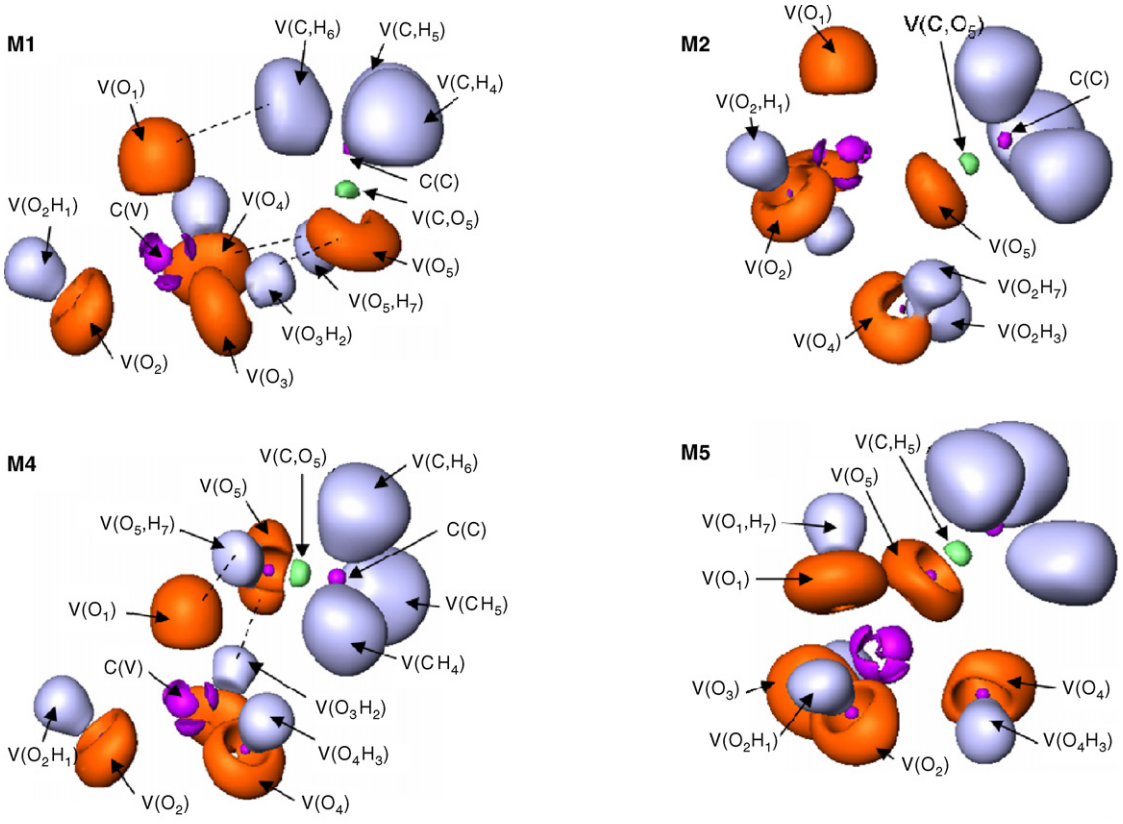

Fig. 4. ELF isosurfaces at $\eta = 0.81$ for **M1**, **M2**, **M4** and **M5**.

Table 2
ELF basin populations $\bar{N}$, and charge transfer (δq) from the catalyst toward the methanol fragments in the hydrated model, calculated at the corresponding B3LYP/6-311G(2d,p) optimized geometry

Basin, $\bar{N}$	M1	M2	M3	M4	M5
C (V)	19.62	19.66	19.87	19.84	19.81
$V(O_1)$	7.18	6.97	6.97	7.04	5.86
$V(O_2)$	6.01	5.89	5.89	5.87	5.87
$V(O_3)$	5.99	5.90	5.90	5.87	5.81
$V(O_4)$	5.89	4.52	–	5.84	5.81
$V(O_2H_1)$	1.68	1.70	1.68	1.68	1.70
$V(O_3H_2)$	1.70	1.75	1.68	1.68	1.70
$V(O_4H_3)$	1.69	1.66	–	1.70	1.71
$V(CH_4)$	2.03	1.99	2.03	2.03	2.03
$V(CH_5)$	2.03	1.99	2.03	2.05	2.03
$V(CH_6)$	2.05	2.03	2.04	2.04	2.03
$V(O_5C)$	1.22	1.28	1.27	1.22	1.32
$V(O_5)$	4.68	6.18	6.10	4.69	5.97
$V(O_5H_7)$	1.76	–	–	1.73	–
$V(O_4H_7)$	–	1.72	–	–	–
$V(O_1H_7)$	–	–	–	–	1.67
δq	−0.03	−0.37	−0.34	−0.03	−0.41

analysis data is presented, namely, the basin populations $\bar{N}$, and the net charge transfer (δq) from the catalyst toward the methanol fragments.

On the basis of the topological ELF analysis, all V–O bonds belong to the unshared-electron type dominated by the electrostatic interactions, and the lack of disynaptic V(V,O) basins allows us to consider an ionic interaction of vanadium and oxygen atoms as in previous studies of VO_x systems reported by Calatayud et al. [36] In other words, all the V–O bonds including the vanadyl V=O species are mainly of ionic character. The shorter V=O distance does not correspond to a covalent bond but rather to a stronger ionic bond [37–39]. As can be seen in Table 2, the oxygen atom in the vanadyl group presents higher population, ∼7*e*, than those in the hydroxyl groups, ∼6*e*. The methanol molecule presents a covalent bond between C and O (green basin $V(C,O_5)$) atoms. The C–H or O–H bonds are covalent but no disynaptic basin is found between the two centers. This is due to the absence of core electrons in the hydrogen center.

The molecular interaction of methanol with the vanadate substrate (structures **M1** and **M4**) is weak and of electrostatic character. This can be seen in Fig. 3 by the absence of disynaptic basin between the two moieties (dashed line). There is a small amount of charge density transfer from the catalyst to the methanol (−0.03*e*) in the initial stage of the adsorption for Path 1 and Path 2. The methoxy species are characterized by a charge density transfer δq of −0.37*e* (**M1**), −0.37*e* (**M2**) and −0.41*e* (**M5**) respectively when the CH_3O– fragment is bonded to the vanadium center. Also, the vanadyl oxygen atoms possess higher density in the molecular systems (7.18*e*, 7.04*e* for **M1** and **M2**, respectively) than in the dissociated ones (6.97*e* for **M2**, **M3** and 5.96*e* for **M5**) due to the electron withdrawing effect of the methoxy group. As a consequence the ionic vanadyl bond is shortened and the corresponding vibrational frequencies shift to higher wavenumbers.

Protonation on the vanadyl oxygen O_1 to form **M5** implies that the large population of $V(O_1)$ in the previous reaction complexes, i.e. 7.18*e*, has decreased to 5.86*e* and 5.95*e*, respectively, by the appearance of a new protonated valence disynaptic basin $V(O_1H_7)$. A similar behaviour is found in **M2** methoxy intermediates, where the large population of $V(O_4)$ decreases with regard to previous reaction complexes to 4.52*e* and 4.56*e*, respectively, by the appearance of a new protonated valence disynaptic basin $V(O_4H_7)$.

In all systems the charge of the vanadium atom slightly oscillates between the molecular and dissociated forms. However, it is observed an increase in the core basin of −0.21 electrons between **M2** and **M3**, due to the release of the water molecule.

4. Conclusions

Methanol interaction with isolated vanadate groups has been modelled by means of hybrid B3LYP calculations. Hydrated and titania-supported vanadate groups are represented by a $OV(OH)_3$ and $OV(OTiO_2H)_3$ clusters that account for the tetrahedral coordination and V oxidation state of vanadium in real catalysts. Molecular and dissociative adsorptions have been considered and the intermediates have been characterized as regards geometry, energetics, vibrational spectra and chemical bonding.

Our results show that methanol molecular adsorption depends on hydration: it takes place mainly by hydrogen bonds involving vanadyl groups and hydroxyl species in hydrated conditions, while an acid/base interaction between the vanadium center and the methanol OH group is observed for the supported model. Dissociation is thermodynamically favoured in both cases and takes place via a proton transfer to hydroxyl group or V–O–Ti site forming a $V–OCH_3$ species, with barriers of 16.6 kcal/mol and 13.6 kcal/mol, respectively. The proton transfer to the vanadyl bond presents a higher barrier of 35.3 kcal/mol and 28.6 kcal/mol, respectively and they can thus be discarded. Neither the barriers nor the relative stability are significantly affected by the temperature.

Harmonic vibrational spectra have been calculated for the molecular and dissociated species and a reasonable agreement with previous experimental results is found. Methoxy groups are found to vibrate 10 cm^{-1} lower than the corresponding molecular species. On the contrary, in the presence of methoxy groups the vanadyl vibrations are shifted to higher frequencies. This is explained by the electron withdrawing effect of the methoxy group: the value of transferred charge from the catalyst to the methanol (methoxy) group is −0.03*e* (−0.34*e*).

Acknowledgements

Computational facilities by CCR, IDRIS and CINES are acknowledged. This work was supported by the MEC, DGICYT, CTQ2006-15447-C02-01, Generalitat Valenciana (Projects ACOMP06/122 and GV2007/106). P. GN. is grateful to the HPC program for a research exchange and the MEC for a doctoral fellowship. L.G. thanks to GV for providing a Postdoctoral grant (APOSTD07).

References

[1] M. Badlani, I.E. Wachs, Catal. Lett. 75 (2001) 137.
[2] J.L. Bronkema, D.C. Leo, A.T. Bell, J. Phys. Chem. C 111 (2007) 14530.
[3] L.J. Burcham, L.E. Briand, I.E. Wachs, Langmuir 17 (2001) 6175.
[4] L.J. Burcham, G.T. Deo, X.T. Gao, I.E. Wachs, Top. Catal. 11 (2000) 85.
[5] G. Deo, I.E. Wachs, J. Catal. 146 (1994) 323.
[6] J. Döbler, M. Pritzsche, J. Sauer, J. Am. Chem. Soc. 127 (2005) 10861.
[7] A. Goodrow, A.T. Bell, J. Phys. Chem. C 111 (2007) 14753.
[8] R.Z. Khaliullin, A.T. Bell, J. Phys. Chem. B 106 (2002) 7832.
[9] N.U. Zhanpeisov, Res. Chem. Interm. 30 (2004) 133.
[10] M. Engeser, D. Schröder, H. Schwarz, Chem. -Eur. J. 17 (2007) 2454.
[11] D. Schröder, M. Engeser, H. Schwartz, E.C.E. Rosenthal, J. Döbler, J. Sauer, Inorg. Chem. 45 (2006) 6235.
[12] T. Waters, G.N. Khairallah, S.A.S.Y. Wimala, Y.C. Ang, R.A.J. O'Hair, A.G. Wedd, Chem. Commun. 43 (2006) 4503.
[13] T. Waters, A.G. Wedd, R.A.J. O'Hair, Chem. -Eur. J. 13 (2007) 8818.
[14] B. Silvi, A. Savin, Nature 371 (1994) 683.
[15] M.J. Frisch, G.W. Trucks, H.B. Schlegel, G.E. Scuseria, M.A. Robb, J.R. Cheeseman, J. Montgomery, T. Vreven, K.N. Kudin, J.C. Burant, J.M. Millam, S.S. Iyengar, J. Tomasi, V. Barone, B. Mennucci, M. Cossi, G. Scalmani, N. Rega, G.A. Petersson, H. Nakatsuji, M. Hada, M. Ehara, K. Toyota, R. Fukuda, J. Hasegawa, M. Ishida, T. Nakajima, Y. Honda, O. Kitao, H. Nakai, M. Klene, X. Li, J.E. Knox, H.P. Hratchian, J.B. Cross, C. Adamo, J. Jaramillo, R. Gomperts, R.E. Stratmann, O. Yazyev, A.J. Austin, R. Cammi, C. Pomelli, J.W. Ochterski, P.Y. Ayala, K. Morokuma, G.A. Voth, P. Salvador, J.J. Dannenberg, V.G. Zakrzewski, S. Dapprich, A.D. Daniels, M.C. Strain, O. Farkas,

D.K. Malick, A.D. Rabuck, K. Raghavachari, J.B. Foresman, J.V. Ortiz, Q. Cui, A.G. Baboul, S. Clifford, J. Cioslowski, B.B. Stefanov, G. Liu, A. Liashenko, P. Piskorz, I. Komaromi, R.L. Martin, D.J. Fox, T. Keith, M.A. Al-Laham, C.Y. Peng, A. Nanayakkara, M. Challacombe, P.M.W. Gill, B. Johnson, W. Chen, M.W. Wong, C. Gonzalez, J.A. Pople, Gaussian 03 (Revision B.04), Gaussian, Inc., Pittsburg, PA, 2003.
[16] A.D. Becke, J. Chem. Phys. 98 (1993) 5648.
[17] C. Lee, R.G. Yang, R.G. Parr, Phys. Rev. B 37 (1988) 785.
[18] J.A. Pople, M. Headgordon, K. Raghavachari, J. Chem. Phys. 87 (1987) 5968.
[19] L. Gracia, J. Andres, J.R. Sambrano, V.S. Safont, A. Beltrán, Organometallics 23 (2004) 730.
[20] L. Gracia, V. Polo, J.R. Sambrano, J. Andrés, J. Phys. Chem. A 112 (2008) 1808.
[21] L. Gracia, J.R. Sambrano, J. Andres, A. Beltran, Organometallics 25 (2006) 1643.
[22] L. Gracia, J.R. Sambrano, V.S. Safont, M. Calatayud, A. Beltran, J. Andres, J. Phys. Chem. A 107 (2003) 3107.
[23] H.B. Schlegel, J. Comput. Chem. 3 (1982) 214.
[24] K. Fukui, J. Phys. Chem. 74 (1970) 4161.
[25] C. González, H.B. Schlegel, J. Chem. Phys. 90 (1989) 2154.
[26] C. González, H.B. Schlegel, J. Phys. Chem. 94 (1990) 5523.
[27] P.W. Atkins, J. De Paula, Physical Chemistry, publisher: W.H. Freeman, New York, 2002.
[28] D. Chandler, Introduction To Modern Statistical Mechanics, Oxford University Press, New York, 1987.
[29] D.A. McQuarrie, Statistical Mechanics, University Science Books, Sausalito, CA, 2000.
[30] J.W. Ochterski, Thermochemistry in Gaussian, Gaussian Inc., Pittsburg, PA, 2000.
[31] A.D. Becke, K.E. Edgecombe, J. Chem. Phys. 92 (1990) 5397.
[32] S.N. Noury, X. Krokidis, F. Fuster, B. Silvi, Comput. Chem. 23 (1999) 597.
[33] Amira 3.0, Concepts I-V Indeed -Visual Concepts, Berlin, 2003.
[34] J.N.J. van Lingen, O.L.J. Gijzernan, B.M. Weckhuysen, J.H. van Lenthe, J. Catal. 239 (2006) 34.
[35] M. Calatayud, C. Minot, J. Phys. Chem. C 111 (2007) 6411.
[36] M. Calatayud, S. Berski, A. Beltran, J. Andres, Theor. Chem. Acc. 108 (2002) 12.
[37] B. Silvi, A. Savin, J.Y. Kempf, G. von Schnering, Bull. Pol. Acad. Sci. Chem. 42 (1994) 413.
[38] M. Calatayud, J. Andrés, A. Beltrán, J. Phys. Chem. A 105 (2001) 9760.
[39] M. Calatayud, B. Silvi, J. Andrés, A. Beltrán, Chem. Phys. Lett. 333 (2001) 493.